17th World Conference on Earthquake Engineering, 17WCEE
Sendai, Japan - September 13th to 18th 2020

ESTIMATION OF UNCERTAINTY IN DYNAMIC ANALYSIS APPLIED TO NON-LINEAR RESPONSE OF A SOIL-STRUCTURE SYSTEM

S. Higuchi

Obayashi Co., shunichi.higuchi@obayashi.co.jp

Abstract

As background of general application of dynamic analyses to seismic design in recent years, necessity of validation in numerical code in terms of both initial modeling and non-linear element responses is recognized.

Quantification of uncertainties, which relate with design safety factors, in numerical analyses is required as a sufficient condition for actual structural design, in contrast with traditional examples of code validation, which were mainly focused on a necessary condition with regard to experimental results.

Followings are described in this paper.

(1) Code validation, utilizing 2D dynamic effective stress FEM code O-EFECT, was conducted targeting on dynamic centrifuge experiment result regarding the piled foundation built in liquefiable sandy ground performed with various input motions as a validation example.

(2) Parameter studies with respect to properties of ground material were performed to estimate dispersion of prediction performance of the code as quantification of uncertainties.

Keywords: Numerical simulation, Dynamic response, Soil-structure interaction, Uncertainty, Dynamic centrifuge

1. Introduction

In recent years, the need for V&V (Verification and Validation) for engineering simulation has been recognized against the background of generalization of high-performance computers. For example, the American Society of Mechanical Engineers (ASME) has been working on the establishment of V&V standards since 2001 and has held annual V&V symposiums since 2012 to collect opinions and exchange information related to the standards. This is because V&V is identified as a framework for trusting the calculation results to users and society (ensuring credibility) when using numerical simulation for decision making such as design work [1].

The Japan Society of Civil Engineers has an approach to V&V on numerical analysis in the concrete field, as well as the "Subcommittee on V&V in numerical analysis in the civil engineering field" by the Applied Mechanics Committee. The latter gathered many participants in the V&V research workshop held at the 2015 and 2017 JSCE annual meetings, showing high interest in V&V [2]. As the application of seismic response analysis is becoming more common in seismic design and its verification practice, the Earthquake Engineering Committee has initiated “Research Subcommittee on Systematization of V&V on Nonlinear Seismic Response Analysis Method for Ground and Structures” (EEC V&V subcommittee, hereafter) in 2017, and has been working on organizing V&V issues, and systematizing philosophy aiming on its practical development [3].

This study is one of case studies conducted in the activities of EEC V&V subcommittee above. Example evaluation was performed targeting on the centrifugal model experiment results in terms of non-linear response of pile foundations in liquefied ground. Evaluations were focused on followings. (1) The initial model setting and verification of the reproducibility against the experiment results. (2) The predicted performance range against the experimental values when the ground model settings vary.

2. Outline of Experiments Targeted for Analysis

The analyses target was the centrifuge shaking table tests (Fig. 1: Scale 1/25) on the pile foundation structure in the liquefied ground conducted previously by the authors [4]. In this experiment, as shown in Table 1 and Fig. 2, ground and structure responses with different excitation levels (same waveform) were obtained. Because large excitation (equivalent to prototype scale input acceleration of 6.0m/s^2) was applied to the model, liquefaction of the ground and plasticization of RC model piles (cracking of concrete and yielding of reinforcing bars) have been observed.

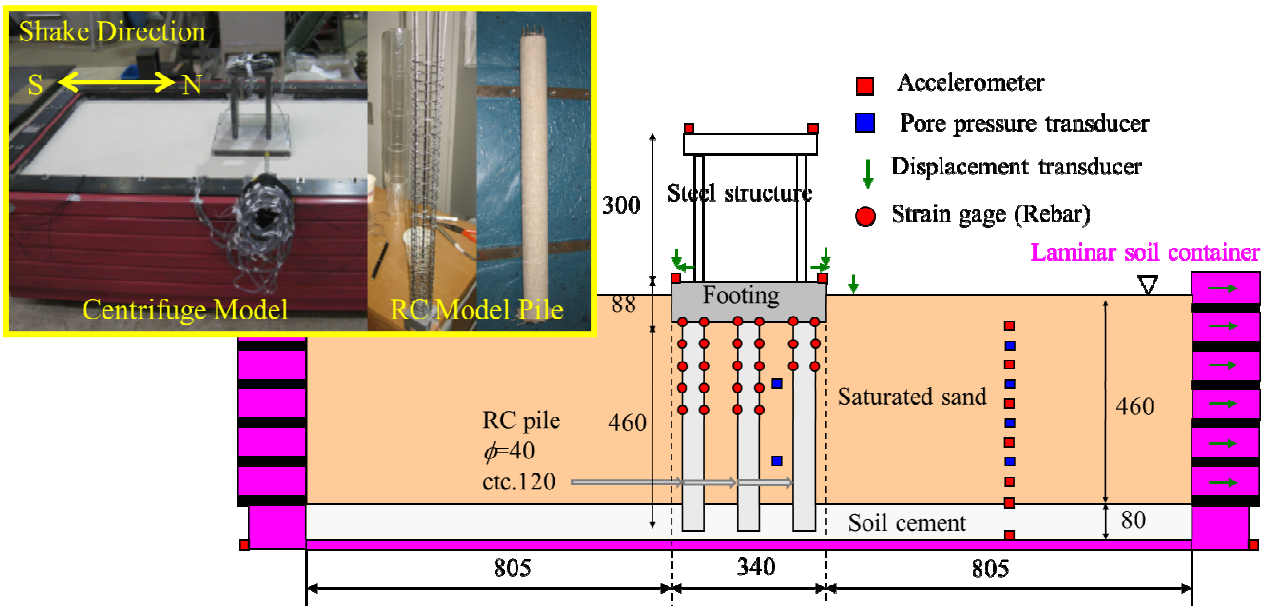

Fig. 1 – Profile of centrifuge model: Scale 1/25 (Unit:mm)

Table 1 – Case of centrifuge experiment and input motion amplitude (Model (Prototype))

Case	d3 (small)	d4 (medium)	d5 (large)
Max. acc. (m/s^2)	25 (1.0)	75 (3.0)	150 (6.0)

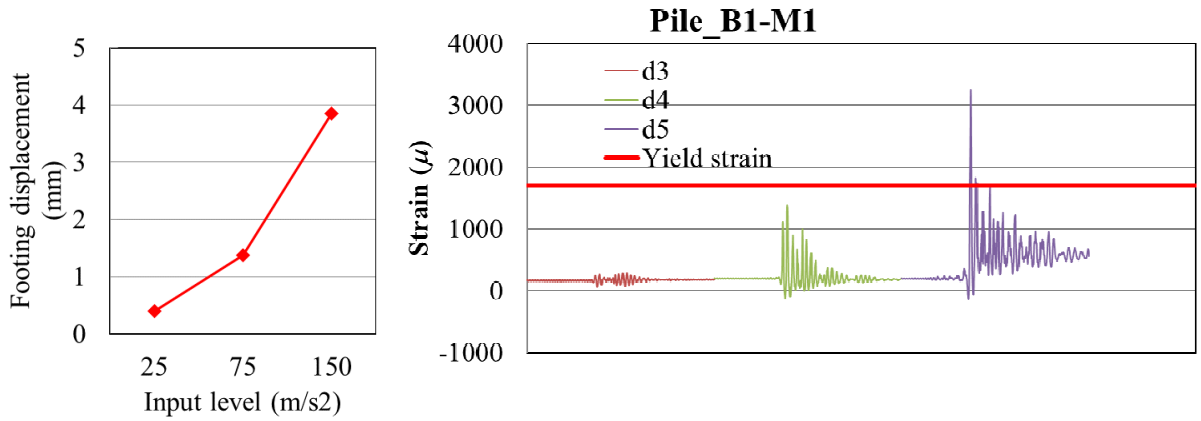

(a) Maximum displacement of footing (b) Observed bar strain time histories

Fig. 2 –Summaries of centrifuge experiment results

3. Verification Analysis

3.1 Analysis method

The verification analysis was conducted by two-dimensional effective stress analysis. The dynamic effective stress analysis program O-EFECT [5] used in this study is based on Biot's multidimensional consolidation theory for saturated porous media that strictly evaluates the coupled effects of soil skeleton and pore water [6]. The ground constitutive model, which introduces parameters that allow repeated loading, is proposed by Matsuoka et.al [7]. For structural modeling, foundation piles are modeled with fiber elements considering the nonlinearity of reinforced concrete and rebar [8, 9], to attempt reproducing pile damage due to seismic effect.

Details on the analytical model (Fig. 3 (a)) were previously given in Ref. [4]. In this study, we firstly verified the component responses reflecting the respective material properties, as shown in Fig.3. The soil element's liquefaction simulation shown in (b) and the model pile loading test simulation shown in (c) were carried out to verify the validity of the numerical code to begin with.

Secondary, as verification of the whole system for the results of the centrifugal model experiment with different excitation levels described in Section 2, focusing on followings, as (i) Verification of the accuracy of the initial structural model and (ii) Verification of the reproducibility of the damage mode. The analysis was performed on a model scale. This is because phenomena related to measurement accuracy, etc. in centrifuge model experiments may not be discriminated by conversion to actual phenomenon.

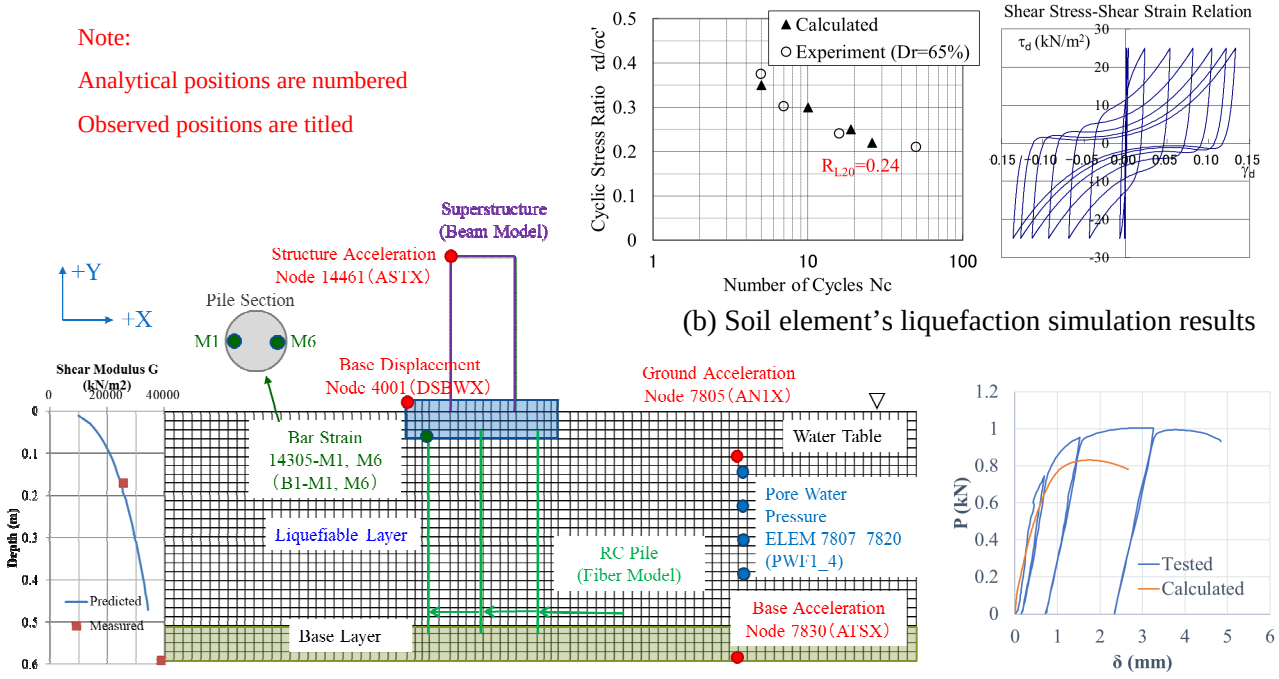

(b) Soil element's liquefaction simulation results

(a) Profile of 2D FE model and representitive observation/extract positions for verification

(c) Model pile loading test simulation results

Fig. 3 – Summaries of analytical model

3.2 Verification of initial structural model

The verification of the initial structural model was performed targeted the small excitation test, at which the ground response equivalent to input acceleration of 10m/s^2 (acceleration of 0.2m/s^2 in actual scale; input acceleration is described by experimental values, hereafter.). At this time, the ground is assumed to be linear,

and the damping constant is set with trial calculations so that the acceleration response (experimental value: red/analytical value: blue) in Fig. 4 (a) consistent.

As shown in Fig. 4 (b), there is good agreement between the acceleration transfer function (ground surface/input: blue line) of the initial ground model according to the estimation relation, determined by the shear wave velocity Vs of the model ground [10], and the observed value (red line: peak frequency f=54Hz) by the experiment. The damping constant identified by trial calculation is h=0.05 for the ground and h=0.01 for the structure, respectively.

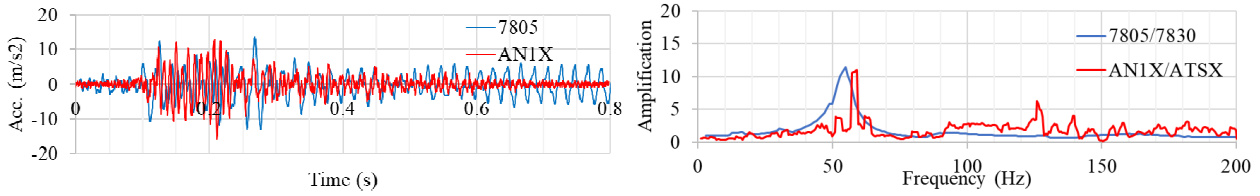

(a) Acceleration time histories (b) Transfer functions

Fig. 4 – Verification results of initial structural model (Ground response)

3.3 Verification of damage mode

The reproducibility of the damage mode was verified by setting the non-linearity of the model ground and applying small (d3:25m/s^2), medium (d4:75m/s^2) and large (d5:150m/s^2) excitations. An example of input earthquake motion time history is shown in Fig.5. All excitation simulations were performed by the same waveform.

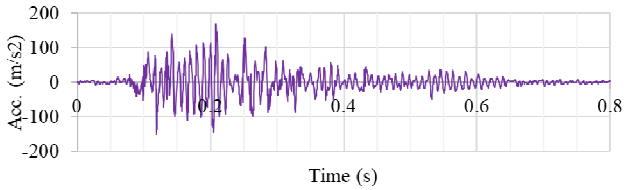

Fig. 5 – Example input earthquake motion time history (Base acceleration, d5)

Fig. 6 shows the acceleration time history, footing displacement time history, and excess pore water pressure ratio time history extracted as items to evaluate the reproducibility of the experiment and compared with the experimental results. The extracted values are red for experimental values and blue for analytical values. Data extraction positions are previously shown in Fig. 3.

3.3.1 Acceleration time history

From the time history of acceleration at the top of the structure in each case shown in Fig. 6 (i), it is observed that the magnitude and phase of the response acceleration are almost consistent in each excitation. In the experimental values for medium and large excitations, short-period responses appear, and similar responses are also observed in the ground acceleration (ii).

The ground acceleration (ii) has a base peak acceleration of 25 m/s^2 with small excitation, while the peak response near the ground surface is 20m/s^2 and the amplitude ratio is about 1 for both experimental and analytical values. On the other hand, with medium excitation, amplitude ratio of the ground is 1/3 with respect to the base motion, and the characteristics of the liquefied ground appeared. In the case of large excitation, the maximum experimental value is 100m /s^2 (excluding t=0.15s spike) while the maximum value is 20m/s^2 in the analysis.

(i) acceleration of top of the structure

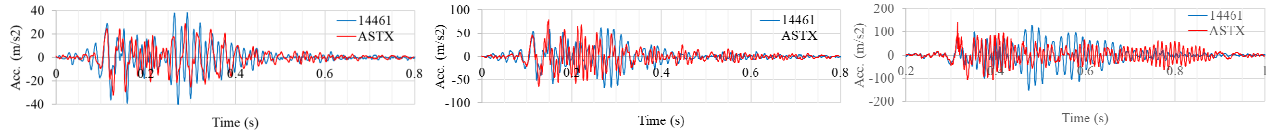

(ii) Ground acceleration

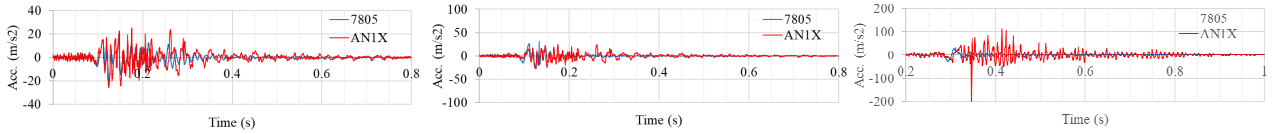

(iii) Horizontal displacement of the footing

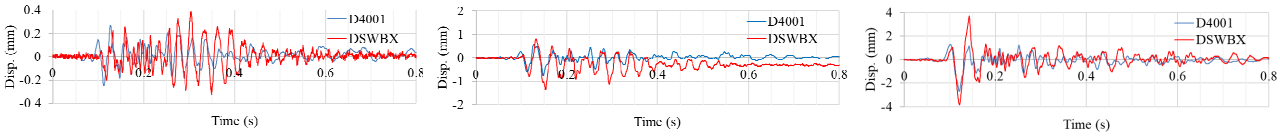

(iv) Excess pore water pressure ratio of ground (shallow position)

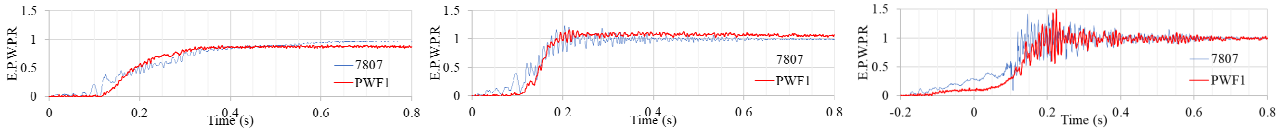

(v) Excess pore water pressure ratio of ground (deep position)

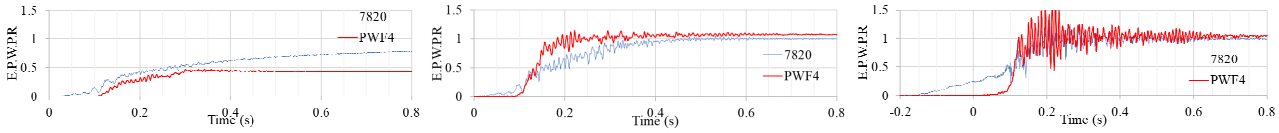

(a) small shake (d3) (b) Medium shake (d4) (c) Large shake (d5)

Fig. 6 – Comparison of observed and analyzed time histories by shake events

Focusing on the large excitation responses, comparing these with the excess pore water pressure ratio time histories shown in Fig. 6 (iv) and (v), it is observed that the acceleration amplitude does not increase at the time when the ground liquefies over all deposit. This is the typical characteristics of the acceleration response of the liquefied ground in seismic observation at site [11].

3.3.2 Footing displacement time history

The horizontal displacement time histories of the footing shown in Fig. 6 (iii) increase in magnitude according to the excitation level, and consistency are observed in terms of both amplitude order and phase in wave form on the experimental results and the analytical results. In small excitation, the analysis value is large in the latter half of the excitation, because of the degree of ground liquefaction differs between experiment and analysis. On the other hand, when the ground is liquefied, the maximum response values in the analyses are only 60% to 70% of the experimental values.

3.3.3 Excess pore water pressure ratio time history

In the excess pore water pressure ratio time histories shown in Fig. 6 (iv) and (v), liquefaction of whole deposit occurs at time t=0.2s for both experimental and analytical values of medium and large excitations. In addition, the generation of large dynamic excess pore water pressure has been reproduced under large excitation. In the case of small excitation, the water pressure continues to increase in the deep ground even

after the time t=0.5s. For large excitation, the time history is shown for the interval of -0.2s-0.8s because the generation time of excess pore water pressure starts earlier than small and medium excitation. This is due to the amplitude of minor motion before the main motion included in the excitation wave enlarged as the amplitude factor of the original motion increases as well.

3.3.4 Repeatability of pile damage mode

Fig. 7 compares the foundation pile/pile head reinforcement strain response in medium and large excitations. The comparison position is the rebar located just below the footing of the left pile (B1 pile). As for the reinforcing bar strain data process, the initial value is not set to zero in each excitation (the amplitude is not incrementally evaluated), because of the necessity to judge the yield of rebar. In other words, the initial value of the experimental value shown here is the initial stress due to centrifugal loading or the initial strain reflecting the seismic excitation history, whereas the analytical value is the initial strain reflecting only the initial stress analysis result without the seismic excitation history.

In the case of medium excitation, strains exceeding 1,000μ were observed at the left edge of the pile (B1-M1) in the experimental value, whereas in the analysis, the strain (14305-M1) amplitude at almost the same position is small. On the other hand, at the right edge of the pile (B1-M6), a strain waveform (14305-M6) similar in amplitude and phase is seen in the experiment and analysis. This is presumed to be due to the presence or absence of concrete cracks. When cracks developed in the cover concrete near the strain measurement point and initiate crack opening, the strain of the reinforcing bar at that position largely increases. Therefore, it is possible that cracks occurred in the experiment, and the occurrence of large repetitive strains in (B1-M1) observed in the experiment data suggests this.

In large excitation, the experimental and analytical values of the strain response of the rebar are in good agreement with both left and right edges of the pile. Compared with the footing displacement response time history previously shown in Fig. 6 (c) (iii), the maximum strain occurrence time t=0.124s coincides with

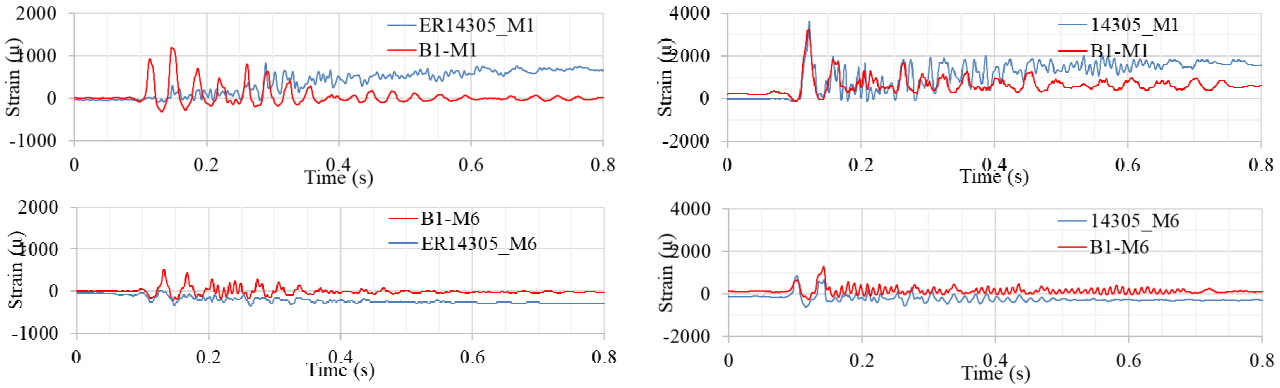

(a) Medium shake (d4) (b) Large shake (d5)

Fig. 7 – Comparison of observed and analyzed time histories on pile head bar strain

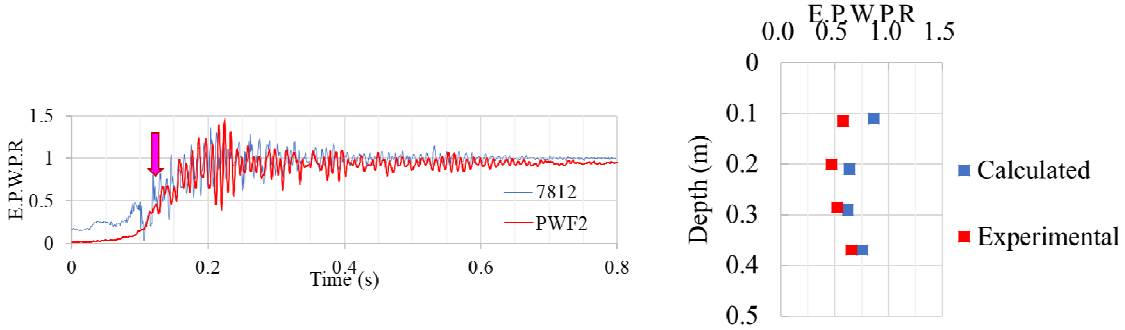

Fig. 8 – Excess pore water pressure distribution in ground at t=0.124s (Large shake)

the maximum displacement time of the leftward footing movement. In addition, rebars yield in the experiment and analysis as the magnitude of the experimental value (B1-M1) of 3,250μ, and the analysis value (14305-M1) of 3,600μ, respectively.

On the other hand, the maximum strain occurrence time t=0.145s at the right edge of the pile, which corresponds to the maximum displacement time of the footing movement in the rightward, yielding is not observed in experimental value (B1-M6) 1,200μ . Maximum strain of the analytical value (14305-M6) is observed at t=0.102s as 850μ, instead. At the time t=0.145s, the analytical value (14305-M6) is 600μ due to deviation occurred toward compresstion strain. Note that, as described above, because the rebar strain at the time of large excitation starts from the accumulated value due to past seismic excitation histories, there is a larger deviation from the analysis value.

Judging from the time history of excess pore water pressure and its distribution in depth, as shown in Fig. 8, at the time of t=0.124s, which correspond to the maximum strain of the reinforcing bar and its yield, it is observed that the excess pore pressure ratio stayed lower than 1 throughout liquefiable deposit. In other words, the damage mode appeared in the pile without complete ground liquefaction.

Fig. 9 shows the maximum strain distribution of rebars of B1 pile in terms of the ground depth from Large shake. Both calculated and observed values are plotted together for comparison. As it is seen that reproductivity of rebar strain distribution of B1 pile is also confirmed.

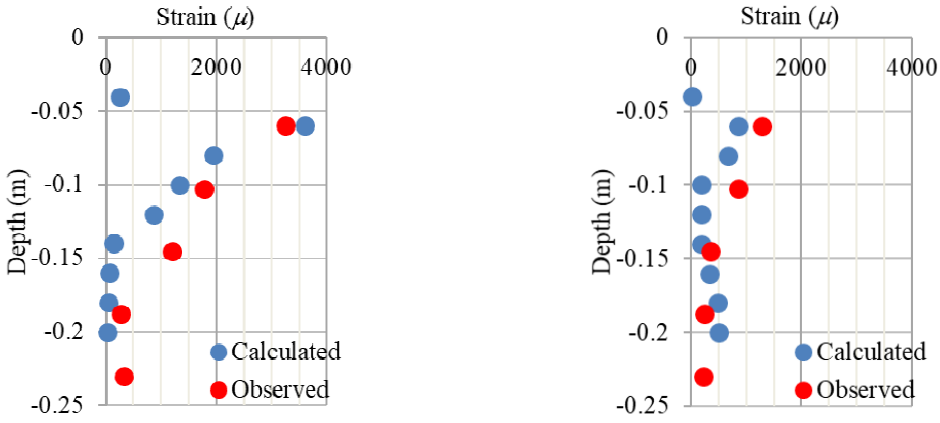

(a) Rebar strain M1 - M5 (Left side of the pile) (b) Rebar strain M6 – M10 (Right side of the pile)

Fig. 9 - Maximum strain distribution of rebars of B1 pile in terms of the ground depth

3.3.4 Group pile effect

The strain time history of M1 (the left edge of the pile head) and M6 (the right edge of the pile head) is consistent with the experimental and analytical values for both phase and amplitude even after the maximum amplitude appears. Discussion will be made regarding the features as known as the group pile effect. The group pile effect induces the reduction of the subgrade reaction due to the presence of the piles in front and back of a designated pile. In this case, M1 is at the left edge of the pile and outside the pile foundation, and M6 is at the right edge of the pile and inside the pile foundation. Therefore, when the footing displacement is to the left ward, larger reaction can be expected. On the other hand, in the case of rightward displacement, the ground reaction force will be reduced due to the group pile effect. Consequently, larger counterclockwise bending moment generated at the pile head when the footing displacement in the leftward, and the clockwise bending moment appeared at the pile head is relatively small when the footing displacement in the rightward. This is consistent with the difference in response characteristics of M1 and M6 rebar strains observed in experiments and analyses.

From the above, the reproducibility in the analysis of the damage mode in the centrifugal model experiment is confirmed including a complicated event in which the pile damage occurrence at the time when the ground does not reach liquefaction.

4. Predictive Performance Evaluation Analysis

Investigation on the effects of (i) initial ground stiffness and (ii) liquefaction strength on the predicted performance will be made in this chapter, based on the response value in the large excitation case described above, as a variation of the ground model.

Here, (a) footing displacement and (b) pile head rebar strain is focused on as evaluation items for prediction performance.

4.1 Influence of initial ground stiffness

The initial ground stiffness shown in Table 2 was evaluated. Since the initial ground stiffness of the analysis model was given by the estimated V_s, the coefficient of variation CV=± 0.2 is applied to the reference value (V_{sm}: V_s at the reference constraint pressure σ_{cm}'=100kN/m^2). Note that CV=0.1 in the Seismic PRA Standard of Nuclear Facilities by Atomic Energy Society of Japan [12].

Fig. 10 shows a comparison of response time histories. Followings are observed. (a) There is no difference in footing displacement due to differences in the ground model. (b) Pile head reinforcement strain (B1-M1: left side of section, B1-M6: right side of section) does not show any difference in maximum value. Note that, in case-s2 where the initial shear stiffness is set to a small value, there is a tendency for the transient response strain (green line) amplitude to increase in M1. However, the difference in the strain response of the reinforcing bars does not affect the damage mode of the piles. If the ground is completely liquefied as shown in this case, it is suggested that the effect of variations in the initial ground stiffness may disappear.

Table 2 – Case of evaluation in terms of initial ground stiffness

Case	-s2	N	+s2
Coefficient of variation CV	-0.2	-	+0.2
V_{sm} (m/s)	113	142	170
G_{0m} (kN/m^2)	24,400	38,200	54,900

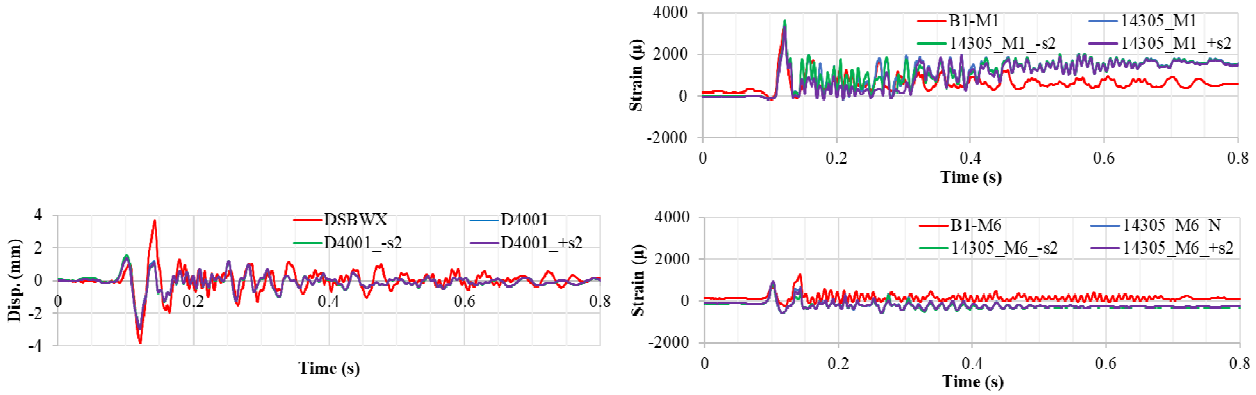

(a) Footing displacement (b) Pile head reinforcement strain

Fig. 10 – Comparison of analyzed time histories in terms of initial ground stiffness

4.2 Effect of liquefaction strength

The influence of liquefaction strength was investigated as valuables of R_{L20}=0.20 and R_{L20}=0.28 set for the reference liquefaction strength, R_{L20}=0.24 (Defined as the shear stress ratio τ_d/σ_c' of 20 cycles of which axial strain of the triaxial specimen exceeds DA5%) for the verification model, as shown in Fig.3. Fig. 11 shows the results of soil element liquefaction test simulation. Note that the liquefaction strength was fitted by changing only the parameter k_s [5], which rules hardening of non-linear stress-strain relation of soil with reference stress condition. Because of stress dependency of k_s, the setting value in the model ground varies depending on the depth as well as V_s or G_0.

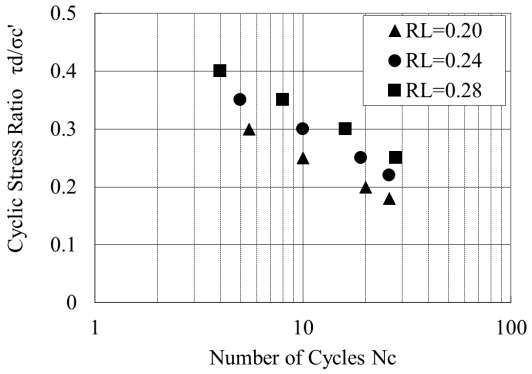

Fig. 11– Results of liquefaction strength element simulation

Fig. 12 shows a comparison of response time histories. Followings are observed. (a) There is no difference in footing displacement due to differences in the ground model. (b) pile head reinforcement strain (B1-M1: left side of section, B1-M6: right side of section) has a difference in maximum value at M1.

It is observed that response strain amplitude is large in case R_{L20}=0.20 (green line) when the liquefaction strength is set small and tends to decrease as case R_{L20}=0.28 (purple line) where the liquefaction strength is set large. The maximum strain of 3,790μ. for RL20=0.20 and 3,250μ. for R_{L20}=0.28 are observed, respectively. In this verification example, the difference in the strain response of the reinforcing bars does not affect the damage mode of the pile, but if the conditions of the structure are different, the variation in liquefaction strength may affect the damage mode.

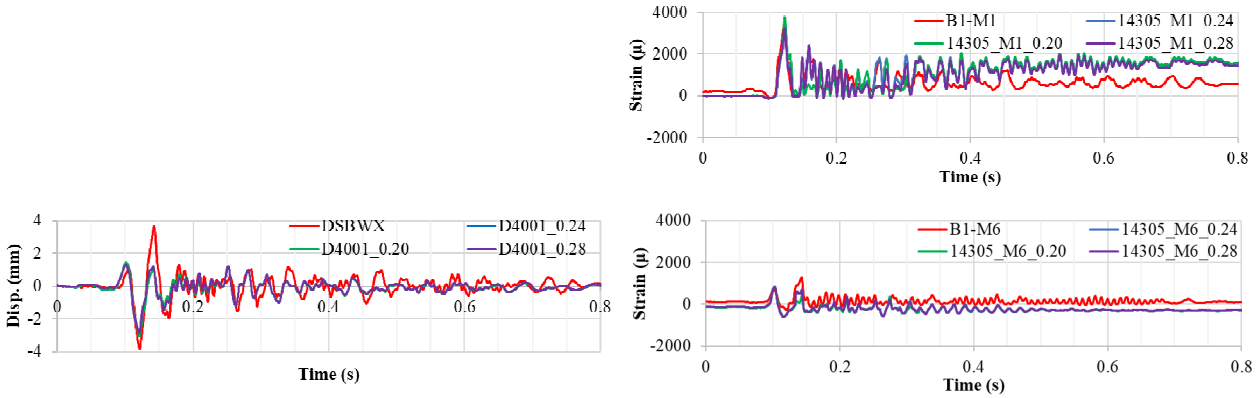

(a) Footing displacement (b) Pile head reinforcement strain

Fig. 12 – Comparison of analyzed time histories in terms of liquefaction strength

5. Conclusion

In this study, the verification of the reproducibility, as well as the evaluation of predicted performance of the non-linear numerical analyses using a centrifugal model experiment of pile foundations in liquefied ground as a target were conducted. The findings obtained are shown below.

a) The reproducibility of the experimental results was evaluated with respect to 4 stage excitations (actual input acceleration of 0.2m/s^2,1.0m/s^2,3.0m/s^2,6.0m/s^2). The reproducibility of the acceleration, displacement and excess ground pore water pressure response were confirmed.

b) As an evaluation of the damage mode, the response of the pile (yield of reinforcing bar) was examined. As a result, the reproducibility with large excitation was satisfactory, but there was a discrepancy with medium excitation. This is presumably due to the presence or absence of cracks in the cover concrete.

c) For the case of large excitation, the experimental results show a complicated event that damages the pile head at a time when the ground does not reach full liquefaction, the reproducibility was confirmed including the group pile effect.

d) As a result of predictive performance evaluation analysis for large excitations, it was suggested that the influence of the variation in initial ground stiffness disappears due to liquefaction of the ground. On the other hand, potential influence on the damage mode was suggested because of a difference in the magnitude of the strain generated in the reinforcement of the foundation pile due to the variation in liquefaction strength.

6. References

[1] Koshimura S, Tanano N, Yamada T, Yoshida Y, Sakurai H, Hasegawa H, Matsui K (2016): Recent development in V&V, *Proceedings of the conference on computational engineering and science*, **21**, JSCES.

[2] http://www.jsce.or.jp/committee/amc/report.html (cited 2019.12.09)

[3] http://committees.jsce.or.jp/eec218/ (cited 2019.12.09)

[4] Higuchi S, Tsutsumiuchi T, Otsuka R, Ito K, Ejiri J (2012): Centrifugal vibration test of RC pile foundation, *Journal of JSCE*, A1, Vol.68, No.4, I_642-I_651.

[5] Ito K (1995): EFECT: The code of effective stress analyses (Part1) - Basic theory and constitutive model of soils -, *Report of obayashi corporation technical research institute*, No.51, 7-14.

[6] Biot M A (1962): Mechanics of deformation and acoustic propagation in porous media, *Journal of Applied Physics*, Vol.33, No.4, 1482-1498.

[7] Matsuoka H, Sakakibara K (1987): A constitutive model for sands and clays evaluating principal stress rotation, *Soils and Foundations*, Vol.27, No.4, 73-88.

[8] Naganuma K (1995): Stress-strain relationship for concrete under triaxial compression, *Journal of struct. const. eng.*, AIJ, Vol.474, 163-174.

[9] Naganuma K, Okubo M (2000): An analytical model for reinforced concrete panels under cyclic stress, *Journal of struct. const. eng.*, AIJ, Vol.536, 135-142.

[10] Sato K (2002): The velocity of S-wave and P-wave measured by bender element at the centrifugal force field, *Proceedings of the annual conference of JSCE*, **3**, Vol.57, 1129-1130.

[11] Sugito M, Sekiguchi K, Yashima A, Oka F, Taguchi Y, Kato Y (1996): Correction of orientation error of borehole strong motion array records obtained during the south hyogo earthquake of Jan. 17, 1995, *Journal of JSCE*, I-34, No.534, 51-63.

[12] Atomic Energy Society of Japan (2007): Standards for probabilistic safety evaluation for nuclear power station caused by earthquakes 2007, AESI-SC-P006.

